

Beam dynamics for LHC upgrades

T. Pugat¹

B. Dalena¹, O. Napolý¹

L. Bonavantura², A. Simona²

R. De Maria³, M. Giovannozzi³, E. Maclean³, J. Molson³,
S. Roussenschuck³, E. Todesco³, R. Tomás³

¹CEA -
DRF/lrfu/DACM/LEDA



²MOX, Politecnico di Milano,
Milano, Italy



³CERN



PhD Thesis: 17 April 2018 - 17 April 2021

Contents

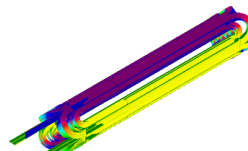
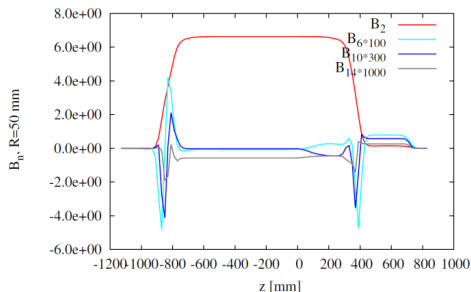
- 1 Thesis project
- 2 Modeling and Simulation
- 3 Test
- 4 Measurements with the beam
- 5 Magnetic Measurements

Contents

- 1 Thesis project
- 2 Modeling and Simulation
- 3 Test
- 4 Measurements with the beam
- 5 Magnetic Measurements

Thesis project

In order to be able to improve the design and performance of future colliders, models of the magnetic fields non-linearities needs deeper understanding. These non-linearities mainly come from magnet fringe fields and ends connections.



Nb₃Sn Quadrupole prototype for HL-LHC
Simulated with ROXIE
Courtesy of CERN magnet group

Goals:

- Develop a "realistic" non-linear transfer map for tracking studies.
- Use calculated or measured magnetic field map given by the magnet designers.
- Define observables sensitive to the longitudinal field description.

Contents

1 Thesis project

2 Modeling and Simulation

- Hamiltonian and Vector potential representation
- 2nd order Lie Integrator
- Step size in z
- Implementation in SixTrack

3 Test

4 Measurements with the beam

5 Magnetic Measurements

Hamiltonian and Vector potential representation

E. Forest (Ref. [1]):

8 D equivalent Hamiltonian of a quadrupole ($a(x, y, z) = q \frac{A(x, y, z)}{P_0 c}$):

$$H[x, p_x, y, p_y, s, \delta, z, p_z; \sigma] = -\sqrt{(1 + \delta)^2 - (p_x - a_x)^2 - (p_y - a_y)^2} + p_z - a_z$$

\Downarrow

$$K[x, p_x, y, p_y, s, \delta, z, p_z; \sigma] = p_z - a_z - \delta + \frac{(p_x - a_x)^2}{2(1 + \delta)} + \frac{(p_y - a_y)^2}{2(1 + \delta)}$$

A. Simona (Ref. [2]), M. Venturini (Ref. [3]) and A.J. Dragt (Ref. [4]):

Generalized Gradient: $C_{m,*}^{[n]}(z) = \frac{i^n}{2^m m!} \frac{1}{\sqrt{2\pi}} \int_{-\infty}^{+\infty} \frac{k^{m+n+1}}{I'_m(Rk)} \hat{B}_{m,*}(R, k) e^{ikz} dk$

Vector potential representation: $A(x, y, z) = \sum_{i,j} x^i y^j c_{ij}(z)$

Gauge:

● **AF:** $A_\phi \equiv 0$

● **HFC:** $\mathbf{A} = \mathbf{A}' + \nabla \lambda$ such that $A_x \equiv 0$ with $\nabla \cdot \mathbf{A} = 0$

Errors in the gradient reconstruction for $R \geq R_{analysis}$

2nd order Lie Integrator

For the position $\mathbf{q} = (x, y, \dots)$ and the momentum $\mathbf{p} = (p_x, p_y, \dots)$:

$$\begin{aligned}
\mathbf{q}^{i+1/13} &= \mathbf{q}^i + \left\{ \begin{array}{ccc} 0, & 0, & \dots \\ 0, & 0, & \dots \\ 0, & 0, & \dots \\ \frac{\Delta\sigma}{2} \frac{p_x^{i+3/13}}{(1+\delta)}, & 0, & \dots \\ 0, & 0, & \dots \\ 0, & 0, & \dots \\ 0, & \Delta\sigma \frac{p_y^{i+6/13}}{(1+\delta)}, & \dots \\ 0, & 0, & \dots \\ 0, & 0, & \dots \\ \frac{\Delta\sigma}{2} \frac{p_x^{i+9/13}}{(1+\delta)}, & 0, & \dots \\ 0, & 0, & \dots \\ 0, & 0, & \dots \\ 0, & 0, & \dots \end{array} \right\} & \mathbf{p}^{i+1/13} &= \mathbf{p}^i + \left\{ \begin{array}{ccc} 0, & 0, & \dots \\ \frac{\Delta\sigma}{2} \frac{\partial a_z^{i+1/13}}{\partial x}, & \frac{\Delta\sigma}{2} \frac{\partial a_z^{i+1/13}}{\partial y}, & \dots \\ -a_x^{i+2/13}, & -\int \frac{\partial a_x^{i+2/13}}{\partial y} dx, & \dots \\ 0, & 0, & \dots \\ a_x^{i+4/13}, & \int \frac{\partial a_x^{i+4/13}}{\partial y} dx, & \dots \\ -\int \frac{\partial a_y^{i+5/13}}{\partial x} dy, & -a_y^{i+5/13}, & \dots \\ 0, & 0, & \dots \\ \int \frac{\partial a_y^{i+7/13}}{\partial x} dy, & a_y^{i+7/13}, & \dots \\ -a_x^{i+8/13}, & -\int \frac{\partial a_x^{i+8/13}}{\partial y} dx, & \dots \\ 0, & 0, & \dots \\ a_x^{i+10/13}, & \int \frac{\partial a_x^{i+10/13}}{\partial y} dx, & \dots \\ \frac{\Delta\sigma}{2} \frac{\partial a_z^{i+11/13}}{\partial x}, & \frac{\Delta\sigma}{2} \frac{\partial a_z^{i+11/13}}{\partial y}, & \dots \\ 0, & 0, & \dots \end{array} \right\}
\end{aligned}$$

2nd order Lie Integrator

For the position $\mathbf{q} = (x, y, \dots)$ and the momentum $\mathbf{p} = (p_x, p_y, \dots)$:

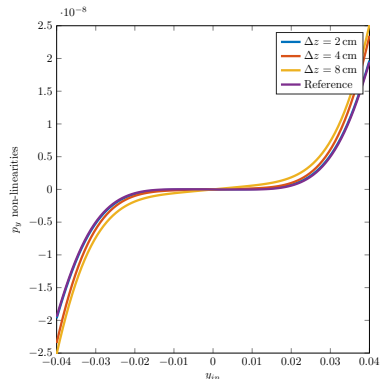
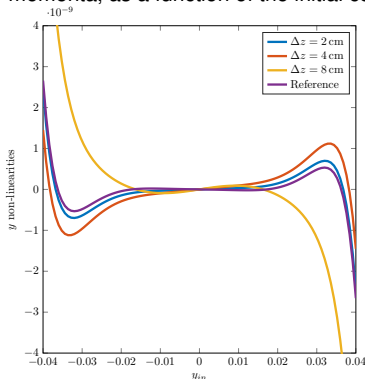
$$\begin{aligned}
 \mathbf{q}^{i+1/13} &= \mathbf{q}^i + \left(\begin{array}{ccc} 0, & 0, & \dots \end{array} \right) & \mathbf{p}^{i+1/13} &= \mathbf{p}^i + \left(\begin{array}{ccc} 0, & 0, & \dots \end{array} \right) \\
 \mathbf{q}^{i+2/13} &= \mathbf{q}^{i+1/13} + \left(\begin{array}{ccc} 0, & 0, & \dots \end{array} \right) & \mathbf{p}^{i+2/13} &= \mathbf{p}^{i+1/13} + \left(\begin{array}{ccc} \frac{\Delta\sigma}{2} \frac{\partial a_z^{i+1/13}}{\partial x}, & \frac{\Delta\sigma}{2} \frac{\partial a_z^{i+1/13}}{\partial y}, & \dots \end{array} \right) \\
 \mathbf{q}^{i+3/13} &= \mathbf{q}^{i+2/13} + \left(\begin{array}{ccc} 0, & 0, & \dots \end{array} \right) & \mathbf{p}^{i+3/13} &= \mathbf{p}^{i+2/13} + \left(\begin{array}{ccc} -a_x^{i+2/13}, & -\int \frac{\partial a_x^{i+2/13}}{\partial y} dx, & \dots \end{array} \right) \\
 \mathbf{q}^{i+4/13} &= \mathbf{q}^{i+3/13} + \left(\begin{array}{ccc} \frac{\Delta\sigma}{2} \frac{p_x^{i+3/13}}{(1+\delta)}, & 0, & \dots \end{array} \right) & \mathbf{p}^{i+4/13} &= \mathbf{p}^{i+3/13} + \left(\begin{array}{ccc} 0, & 0, & \dots \end{array} \right) \\
 \mathbf{q}^{i+5/13} &= \mathbf{q}^{i+4/13} + \left(\begin{array}{ccc} 0, & 0, & \dots \end{array} \right) & \mathbf{p}^{i+5/13} &= \mathbf{p}^{i+4/13} + \left(\begin{array}{ccc} a_x^{i+4/13}, & \int \frac{\partial a_x^{i+4/13}}{\partial y} dx, & \dots \end{array} \right) \\
 \mathbf{q}^{i+6/13} &= \mathbf{q}^{i+5/13} + \left(\begin{array}{ccc} 0, & 0, & \dots \end{array} \right) & \mathbf{p}^{i+6/13} &= \mathbf{p}^{i+5/13} + \left(\begin{array}{ccc} -\int \frac{\partial a_x^{i+5/13}}{\partial x} dy, & -a_y^{i+5/13}, & \dots \end{array} \right) \\
 \mathbf{q}^{i+7/13} &= \mathbf{q}^{i+6/13} + \left(\begin{array}{ccc} 0, & \Delta\sigma \frac{p_y^{i+6/13}}{(1+\delta)}, & \dots \end{array} \right) & \mathbf{p}^{i+7/13} &= \mathbf{p}^{i+6/13} + \left(\begin{array}{ccc} 0, & 0, & \dots \end{array} \right) \\
 \mathbf{q}^{i+8/13} &= \mathbf{q}^{i+7/13} + \left(\begin{array}{ccc} 0, & 0, & \dots \end{array} \right) & \mathbf{p}^{i+8/13} &= \mathbf{p}^{i+7/13} + \left(\begin{array}{ccc} \int \frac{\partial a_y^{i+7/13}}{\partial x} dy, & a_y^{i+7/13}, & \dots \end{array} \right) \\
 \mathbf{q}^{i+9/13} &= \mathbf{q}^{i+8/13} + \left(\begin{array}{ccc} 0, & 0, & \dots \end{array} \right) & \mathbf{p}^{i+9/13} &= \mathbf{p}^{i+8/13} + \left(\begin{array}{ccc} -a_x^{i+8/13}, & -\int \frac{\partial a_x^{i+8/13}}{\partial y} dx, & \dots \end{array} \right) \\
 \mathbf{q}^{i+10/13} &= \mathbf{q}^{i+9/13} + \left(\begin{array}{ccc} \frac{\Delta\sigma}{2} \frac{p_x^{i+9/13}}{(1+\delta)}, & 0, & \dots \end{array} \right) & \mathbf{p}^{i+10/13} &= \mathbf{p}^{i+9/13} + \left(\begin{array}{ccc} 0, & 0, & \dots \end{array} \right) \\
 \mathbf{q}^{i+11/13} &= \mathbf{q}^{i+10/13} + \left(\begin{array}{ccc} 0, & 0, & \dots \end{array} \right) & \mathbf{p}^{i+11/13} &= \mathbf{p}^{i+10/13} + \left(\begin{array}{ccc} a_x^{i+10/13}, & \int \frac{\partial a_x^{i+10/13}}{\partial y} dx, & \dots \end{array} \right) \\
 \mathbf{q}^{i+12/13} &= \mathbf{q}^{i+10/13} + \left(\begin{array}{ccc} 0, & 0, & \dots \end{array} \right) & \mathbf{p}^{i+12/13} &= \mathbf{p}^{i+11/13} + \left(\begin{array}{ccc} \frac{\Delta\sigma}{2} \frac{\partial a_z^{i+11/13}}{\partial x}, & \frac{\Delta\sigma}{2} \frac{\partial a_z^{i+11/13}}{\partial y}, & \dots \end{array} \right) \\
 \mathbf{q}^{i+1} &= \mathbf{q}^{i+12/13} + \left(\begin{array}{ccc} 0, & 0, & \dots \end{array} \right) & \mathbf{p}^{i+1} &= \mathbf{p}^{i+12/13} + \left(\begin{array}{ccc} 0, & 0, & \dots \end{array} \right)
 \end{aligned}$$

In the Hard Edge case ($A_x = A_y = 0$).

Step size in z

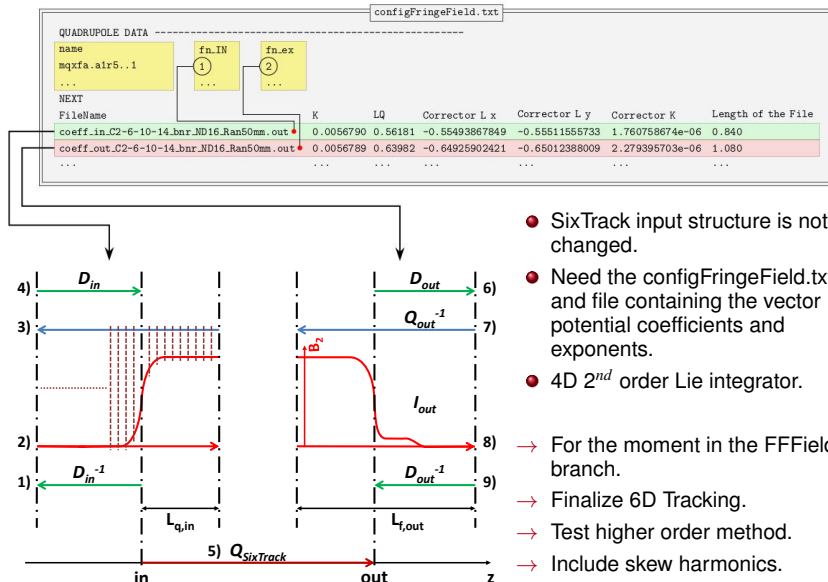
Procedure:

Use different initial position with different offset ($x_{in} = px_{in} = py_{in} = 0$) and only use one quadrupole for the tracking. The linear part is subtracted to the final positions and momenta, as a function of the initial coordinate.



- For a Δz greater than 40 mm, information due to the longitudinal description of the field is greatly deteriorated (Ref. [2] and [5]).

Implementation in SixTrack



- SixTrack input structure is not changed.
 - Need the configFringeField.txt file and file containing the vector potential coefficients and exponents.
 - 4D 2nd order Lie integrator.
- For the moment in the FFField git branch.
- Finalize 6D Tracking.
- Test higher order method.
- Include skew harmonics.

Contents

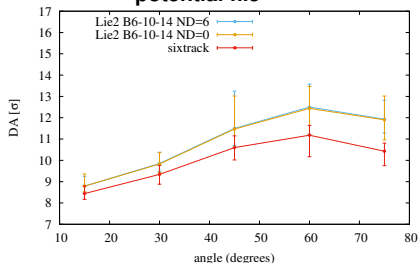
- 1 Thesis project
- 2 Modeling and Simulation
- 3 Test**
 - Dynamic aperture
 - Tune vs Action
 - Single Quad Tracking
- 4 Measurements with the beam
- 5 Magnetic Measurements

Dynamic aperture

Procedure:

- *Particles*: 30 initials conditions for each interval of 2 sigma (0 to 28) and 5 phase-space angles with $\delta = 2.7e^{-4}$.
- *Optic*: HLLHCV1.0 with 60 dipole field errors seeds.
- *Number of revolution*: 10^4 .
- In SixTrack, systematic $b_{6,10,14}$ only are considered and are scaled for the prototype length.

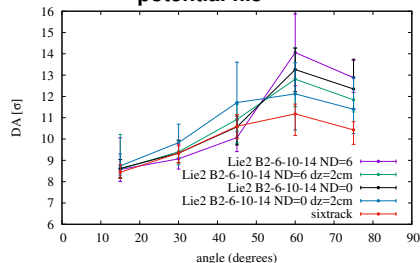
Dynamic aperture without B2 in the vector potential file



Result:

- Effect of the derivatives small compared to effect due to random field errors and to tracking precision.
- SixTrack method is robust against full tracking.

Dynamic aperture with B2 in the vector potential file



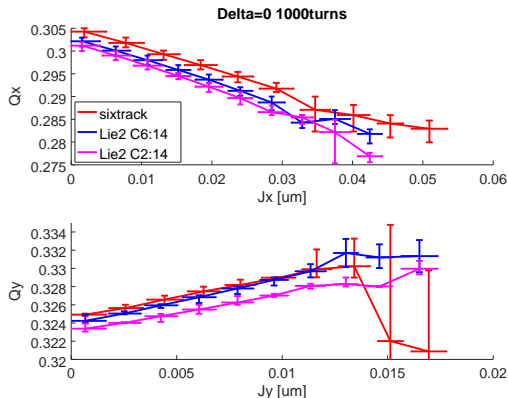
Tune vs Action

Procedure:

- *Particles*: 120 initials conditions with amplitude between 0.033333 mm to 4.000000 mm, the ratio between emittance in the two planes equal to 0.19281 and $\delta = 0$.
- *Optic*: HLLHCV1.0 with only one of the 60 dipole field errors seeds.
- *Number of turns*: 1000.

Result:

- Small systematic between SixTrack and the Lie2 method.
 - Same result for all seeds but covered by random field errors.
 - The small systematic (angle 15°) is not influencing DA result (see previous slide).
- Test different angles.
- Comparison with $dz=2\text{cm}$.



Single Quad Tracking

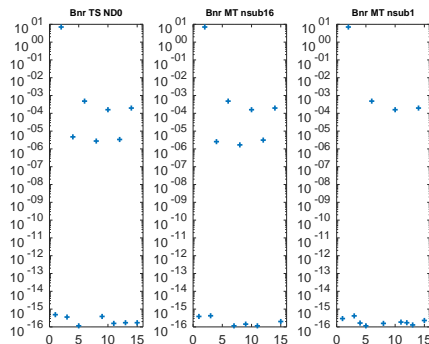
Procedure:

- *Particles*: Initial conditions on a circle for different radius and no transverse momenta.
- *Optic*: Only one quadrupole with a symmetric field. The tracking method is the Lie integrator (TS) with and without derivatives and the SixTrack multipole (MT) with and without subdivision of the thin matrix.
- *Plot*: DFT of the momenta at the end of the Quadrupole.

Result:

- An $b_{4,8,12}$ effect appear in the multipole case when the thin matrix is subdivided.
- This effect increase with the number of subdivision.
- When derivatives are included, the b_4 change sign.
- The additional b_4 increases with the radius.

→ Test with $dz=2\text{cm}$.



Single Quad Tracking

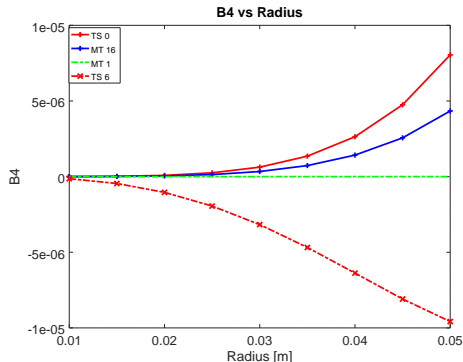
Procedure:

- *Particles*: Initial conditions on a circle for different radius and no transverse momenta.
- *Optic*: Only one quadrupole with a symmetric field. The tracking method is the Lie integrator (TS) with and without derivatives and the SixTrack multipole (MT) with and without subdivision of the thin matrix.
- *Plot*: DFT of the momenta at the end of the Quadrupole.

Result:

- An $b_{4,8,12}$ effect appear in the multipole case when the thin matrix is subdivided.
- This effect increase with the number of subdivision.
- When derivatives are included, the b_4 change sign.
- The additional b_4 increases with the radius.

→ Test with $dz=2\text{cm}$.



Contents

- 1 Thesis project
- 2 Modeling and Simulation
- 3 Test
- 4 Measurements with the beam**
- 5 Magnetic Measurements

Measurements with the beam

Goal:

Search for the signature of non-linear effects in the LHC not described by the present model.

- ✓ July 2017: LHC IR non-linearities studies (E. Maclean, MD 2158)
 - Several measurements and techniques used in LHC to evaluate non linear fields in the IR, using the beams.
 - Measurements of 1^{st} and 2^{nd} order detuning with amplitude.
- ✓ September 2017: LHC IR non-linearities studies (E. Maclean)
 - Measurement of short term DA with AC-dipole.
 - Measurement of long term DA with ADT blow-up.
- Analyse data from the previous MD (1^{st} and 2^{nd} order detuning with amplitudes, ...).
- 2018: Non-linear MDs.
 - We are particularly interested in the b_6 effects of inner triplet.

Contents

- 1 Thesis project
- 2 Modeling and Simulation
- 3 Test
- 4 Measurements with the beam
- 5 Magnetic Measurements**

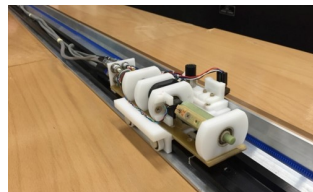
Magnetic Measurements

Goal:

Use computed or measured data for the Tracking and understand the limit of applicability of our model to measured data (filters of noise, measurements precision, etc...).

- **Collaboration with the CERN:** Brief Report of the discussions

- Toy-train measures harmonics in step of micro-meter and provides integrated values on mm longitudinal steps (using a 6 order polynomial) (S. Roussenschuck).
- Consider up to 6 derivatives of the Generalized Gradients in the longitudinal harmonics calculation/measurements (S. Roussenschuck).
- Both integral and "point-like" in z measurements of harmonics (b_n and a_n) can reach a relative resolution of 10^{-6} (S. Roussenschuck).
- For the moment, the prototypes are not representative of the HL-LHC production (E. Todesco).
The possibility to use measurements is not given for the time of the thesis.



- **Collaboration with Fermilab:** ?

Bibliography

- [1] *Explicit symplectic integrator for s-dependent static magnetic field*
Y. K. Wu, E. Forest and D. S. Robin,
in *Phys. Rev. E*, vol. 68, pp. 046502, Oct. 2003.
- [2] *High order time integrators for the simulation of charged particle motion in magnetic quadrupoles*
A. Simona, L. Bonaventura, T. Pognat, B. Dalena,
in arXiv:1802.08157, submitted for publication.
- [3] *Accurate computation of transfer maps from magnetic field data*
M. Venturini, A. J. Dragt,
in *Nucl. Instr. Meth.*, vol. 427, pp. 387-392, May 1999.
- [4] *Lie Methods for Nonlinear Dynamics with Applications to Accelerator Physics*
A. J. Dragt,
University of Maryland, MD, USA, 1997.
- [5] *Calcul d'une "carte de transport" réaliste pour particules chargées*
T. Pognat, B. Dalena,
Technical report. [pdf](#)
- [6] *Accurate and Efficient Tracking in Electromagnetic Quadrupoles*,
T. Pognat *et al.*,
in *Proc. IPAC'18*, Vancouver, Canada, paper THPAK004
- [7] *Fringe Fields Modeling for the High Luminosity LHC Large Aperture quadripôle*,
B. Dalena *et al.*,
in *Proc. IPAC'14*, Dresden, Germany, paper TUPRO002, pp. 993-996. [pdf](#)
- [8] *Construction of higher order symplectic integrators*
H. Yoshida,
in *Phys. Lett. A*, vol. 150, no. 5, pp. 262-268, 1990.

Comparison between Integrator (2,4,6th-Gauss, 4th-RK, 2,4,6th-Lie)

- Lie methods profit more from the change of gauge than the other methods.
- Lie methods are faster with respect to other symplectic methods. The explicit, non-symplectic Runge-Kutta method is the fastest.
- All the methods display the same low accuracy for step size bigger than 4 cm for the realistic field considered.

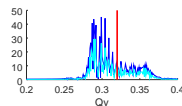
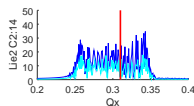
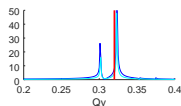
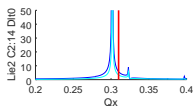
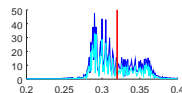
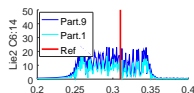
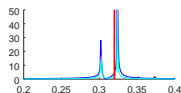
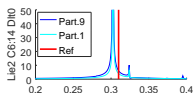
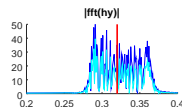
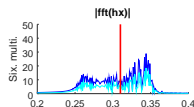
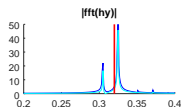
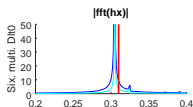
Table: Vector potential evaluation's cost (A. Simona).

	ND=2		ND=16	
	Normal	Skew	Normal	Skew
AF	80	68	352	330
HFC	64	52	251	225
HFC/AF	0.80	0.76	0.72	0.68

Tube Oscillation

Procedure:

- *Particles*: 2 initial conditions with amplitude respectively 0.1993 mm and 0.4599 mm, the ratio between emittance in the two planes equal to 0.19281. In the left plot, $\delta = 0$ and on the right $\delta = 2.7e - 4$.
- *Optic*: HLLHCV1.0 with only 1 dipole field errors seed.
- *Number of turns*: 10^3 .



Tune vs Action

Procedure:

- *Particles*: 120 initials conditions with amplitude between 0.033333 mm to 4.000000 mm, the ratio between emittance in the two planes equal to 0.19281 and $\delta = 0$.
- *Optic*: HLLHCV1.0 with the 60 dipole field errors seeds.
- *Number of turns*: 1000.

Result:

- Small systematic between SixTrack and the Lie2 method.
 - Same result for all seeds but covered by random field errors.
 - The small systematic (angle 15°) is not influencing DA result (see previous slide).
- Test different angles.
- Comparison with $dz=2\text{cm}$.

